Mineral Processing and Extractive Metallurgy Review
An International Journal

ISSN: 0882-7508 (Print) 1547-7401 (Online) Journal homepage: www.tandfonline.com/journals/gmpr20

True flotation *versus* entrainment in reverse cationic flotation for the concentration of iron ore at industrial scale

Virginia P. S. Nykänen, André S. Braga, Thiago C. Souza Pinto, Patricia H. L. S. Matai, Neymayer P. Lima, Laurindo S. Leal Filho & Marisa B. M. Monte

To cite this article: Virginia P. S. Nykänen, André S. Braga, Thiago C. Souza Pinto, Patricia H. L. S. Matai, Neymayer P. Lima, Laurindo S. Leal Filho & Marisa B. M. Monte (2020) True flotation *versus* entrainment in reverse cationic flotation for the concentration of iron ore at industrial scale, Mineral Processing and Extractive Metallurgy Review, 41:1, 11-21, DOI: 10.1080/08827508.2018.1514298

To link to this article: https://doi.org/10.1080/08827508.2018.1514298

MINERAL PROCESSING AND EXTRACTIVE METALLURGY REVIEW
2020, VOL. 41, NO. 1, 11–21
https://doi.org/10.1080/08827508.2018.1514298

Taylor & Francis
Taylor & Francis Group

True flotation *versus* entrainment in reverse cationic flotation for the concentration of iron ore at industrial scale

Virginia P. S. Nykänen[a], André S. Braga [a,b], Thiago C. Souza Pinto[a], Patricia H. L. S. Matai[b], Neymayer P. Lima[c], Laurindo S. Leal Filho[a,b], and Marisa B. M. Monte[a,d]

[a]Instituto Tecnológico Vale, Minas Gerais, Brasil; [b]Laboratory of Transport Phenomena and Chemistry of Interfaces, Department of Mining and Petroleum Engineering, University of São Paulo, São Paulo, Brazil; [c]Vale S.A., Prédio 1, Mina de Águas Claras, Minas Gerais, Brasil; [d]Laboratory for Surface Chemistry, Coordination of Mineral Processing – Center for Mineral Technology, CETEM, Avenida Pedro Calmon, 900, Cidade Universitária, Rio de Janeiro, Brasil

ABSTRACT

The loss of iron-bearing minerals to the tailings, especially in the finest fractions (−44 μm), is a problem that must be endured due to the depletion of deposits containing high-Fe hematite. The two main mechanisms for iron mineral loss in the froth in reverse cationic flotation are hydrodynamic dragging and true flotation. This last one being attributed to failures in the conditioning processes regarding the depression of iron mineral by starch. In this work, two industrial mechanical flotation circuits located in Minas Gerais—Brazil, namely Conceição Itabiritos II and Pico, operating with mineralogically distinct iron minerals, had their tailings analyzed in order to attribute reasons for the iron-bearing minerals losses. Liberation studies excluded losses due to the presence of composite particles where hematite was combined to silica or goethite. The method known as two-liquid flotation was applied to the several particle fractions present in the tailings to evaluate the particles surfaces hydrophobicity/hydrophilicity. The results indicated that for Conceição Itabiritos II, the loss of iron minerals was due to a combination of true flotation and hydrodynamic dragging. True flotation probably took place because of depression failure. For Pico, the results revealed that most of the iron-bearing particles were lost due to hydrodynamic dragging. The shape factor and terminal velocity, both obtained via permeametry, confirmed the two-liquid flotation results. Two-liquid flotation was shown to be a fast and simple method to qualitatively assess the hydrophobicity of particles in froth flotation, thus allowing quick improvements in the process.

KEYWORDS

Flotation; entrainment; true flotation; iron ore

1. Introduction

During the first half of the 20th century iron was recovered primarily from high grade hematite bodies containing over 60 wt% Fe. To date, deposits containing high-Fe hematite have been depleted and the mineral industry needs more often to deal with poorer quality hematite (banded iron formations—BIFs) (Selmi et al. 2009; Gomes et al. 2015). BIFs are mechanically more fragile than typical hematite deposits increasing the amount of fines within the feed. Besides, to recover low-grade minerals, those need to be ground until reaching a certain size to ensure the mineral liberation.

Low-grade iron ores are beneficiated in large scale by froth flotation in the same way as fine size range iron ores (<149 μm) (Lima et al. 2013). Studies related to iron ore flotation began in 1931 and included the direct anionic flotation, and the cationic flotation of quartz, also called reverse cationic flotation. In this process, the gangue mineral, mainly quartz, has its surface modified by a collector becoming hydrophobic, therefore it reported to the froth phase. At same time, iron ore, under the action of a depressant agent, remains hydrophilic at the bottom of the flotation cell. The most common depressant for iron ore is corn starch, due to the satisfactory results delivered, and its great commercial abundance. The mechanism by which starch and hematite interact, in order to avoid the action of collector over the mineral surface, has been extensively discussed and can be checked elsewhere (Peres and Correa 1996; Pavlovic and Brandão 2003). The collectors normally used are etheramines or etherdiamines, which act also as frothers because of their carbon chain (Lima et al. 2013).

The recovery of iron-bearing minerals particles in froth flotation is done either by true flotation or by entrainment (Eisele and Kawatra 2007; Lima et al. 2016). The true flotation refers to the process where particles are led to the froth layer because of the hydrophobicity of their surface (Ross 1991). Commonly, the hydrophobicity of mineral particles is evaluated through contact angle measurements, which involve proper equipment and sample preparation process, depending on the method chosen (Chau 2009).

Entrainment is a physical process where fine particles are dragged to the froth layer, no matter whether their surface is hydrophilic or hydrophobic. These particles enter the lamella

CONTACT Marisa B. M. Monte mmonte@cetem.gov.br Centro de Tecnologia Mineral, Avenida Pedro Calmon, 900, Cidade Universitária, RJ, Rio de Janeiro, Brasil. 21941-908

Color versions of one or more of the figures in the article can be found online at www.tandfonline.com/gmpr.

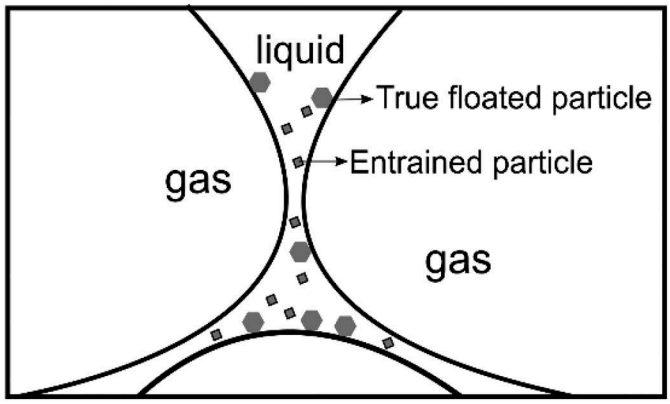

Figure 1. Graphic representation of the entrainment phenomenon. Fine particles are dragged along and become entrapped within the lamellae in the froth. True floated particles are attached to the air bubble by the action of a collector.

of the froth becoming entrapped in this interbubble water layer (Figure 1). The entrainment dilutes the desired material, reducing the grade of the product (Neethling and Cilliers 2009; Wang et al. 2015). The use of a proper froth washing system in flotation cells can decrease the contribution of entrainment in the loss of fine particles; however, those systems are more often a feature of column flotation cells (Kawatra and Eisele 1987; Dowling et al. 2000; Shean and Cilliers 2011).

It is well known that fine particles usually contain the highest amount of iron-bearing minerals lost to the tailings (Gomes et al. 2011). Although fine particles can also take part in true flotation, those tiny particles are especially affected by the entrainment phenomenon, mainly due to their lack of mass. In this context, finding out whether true flotation or entrainment is the predominant reason for valuable mineral loss could improve the operation parameters in order to minimize the loss (Schubert 2008).

The entrainment of particles within the froth layer will depend on many factors; among them are the size and shape of those particles (Wiese et al. 2015). The parameter associated to the shape of particles is the *sphericity* or *shape factor* (ψ), which gives information about how rounded is a determined particle (Mauri 2015). The highest value possible for this parameter, ($\Psi = 1$), corresponds to a perfect sphere (Mauri 2015; Souza Pinto et al. 2016).

Permeametry is a technique that allows us to assess the sphericity of a particle size distribution (Schulz 1974). Permeability is a characteristic parameter of a porous media, being related to the arrangement and distribution of pores by which a given Newtonian fluid must pass through. In the permeametry, a porous media (bed of particles near the same size) is introduced in a close-fitting tube in order to avoid fluid leakage in between the bed of particles and the walls of the tube. This population of particles can have its sphericity determined by the percolation of a gas passing through it, in a laminar flux (Schulz 1974; Eriksson et al. 1990; Souza Pinto et al. 2009).

Two-liquid flotation is a notably useful method to separate fine particles, normally smaller than 10 μm, according to their hydrophobicity (Kocabağ and Güler 2007; Otsuki and Dodbiba 2007). Therefore, this method could evaluate the effectiveness of collector and depressant over a given mineral, during the flotation process. Briefly, this method involves two solvents with different polarities, i.e. polar and nonpolar, which are mixed together with the particles to be separated, forming two phases after ceasing the movement. Particles with hydrophobic surfaces will migrate to the nonpolar phase, attached to the small bubbles of solvent, whereas particles with hydrophilic surfaces will migrate and disperse into the polar phase (Kocabağ and Güler 2007). If the particles present the same surface properties for a particular system, surfactants or other modifying agents can be used to tune the hydrophobic/hydrophilic nature, so that the two-liquid flotation could be used also for those cases. Two-liquid flotation provides fast results using very simple glassware and equipment.

In this work, we analyzed the reasons for iron minerals being recovered from the tailings froth in reverse cationic flotation of iron ore. Two industrial flotation circuits, operating with mineralogically distinct iron ores were object of our studies, using mainly the two-liquid flotation and permeametry to evaluate in a simple, but robust way the source of valuable minerals loss to the tailings. Both sites, Mina do Pico and Mina Conceição Itabiritos II, and their flotation circuits, are located at Minas Gerais, Brazil, in the region known as "Quadrilátero Ferrífero," and they are part of two distinct mineral complexes of iron ore exploitation belonging to the Brazilian mining company Vale S/A.

2. Materials and methods

2.1. Sample collection and preparation

Samples were collected in duplicates on the automatic cutter samplers from the industrial flotation circuits, during a survey of 2 h, with increments being collected every 10 min to compose the final sample. The sampled points on the circuit were: fresh feed, final concentrate, and final tailings. Both circuits operated with conventional flotation machines, with no froth washing system. Samples were sized into three fractions (+105 μm, −105 + 44 μm, −44 μm) for the two-liquid flotation and permeametry experiments. After those procedures, samples from the feed, concentrate, and tailings were sent to chemical and morphological characterization.

2.2. Mineral characterizations

2.2.1. XRF (X-ray fluorescence)

X-ray fluorescence was used to determine the chemical composition of the samples. All the samples were analyzed as melted pellets, and the loss to fire was analyzed by gravimetry, for 1 h at 1050°C.

2.2.2. Mineralogical, chemical, and morphological analyzes

Mineralogical analyzes were done by X-ray diffraction (XRD), using the powder method and a position sensitive detector. Crystalline phases were compared with the following databases: ICDD (International Center for Diffraction Data)—2003 and PANICSD (PANanalytical Inorganic Crystals Structure Database)—2007. Qualitative and semiquantitative evaluation of chemical elements within the samples was

conducted by scanning electron microscopy (SEM)—Stereoscan 400 (LEO)—equipped with an energy dispersion scattering detector (EDS)—Oxford. The analyzed sections were previously sputtered with carbon. Samples having diameters over 20 μm were subject of detailed mineralogical study to determine the mineral occurrence, and the associations of those minerals. The analyses were done by the use of the software MLA—Mineral Liberation Analyzer—(FEI), over polished surfaces of the particles. The software was coupled to a SEM—600 (FEG)—which has also a microanalyses system EDS Espirit—Brucker.

2.2.3. Hydrophobicity test—two-liquid flotation

For the two-liquid flotation experiments, 375 mL of distilled water and 125 mL of isooctane were poured into a 1000 mL beaker, and the mixture was mechanically stirred for 2 min at 1000 ± 20 rpm, to condition the mixture. The rotor size choice followed the relation $D_{beaker} = 3 \times d_{rotor}$, which gave d = 37.08 mm (Froude number = 1.05). These experimental conditions adopted provided a very well homogenous mixture without vortex creation (Arbiter et al. 1976). After the conditioning time, ~ 20 g of a sample taken from the fraction −44 μm (final tailings), were added to the stirring mixture and stirred for 3 min, with that same rotor speed. It is important to point out that the mineral samples must still be humid; not passing by any drying processes prior the experiment, to keep the chemical environment in which the particles were immersed in the industrial cell/tank. The stirring was stopped, and the system was kept untouched for 3 min to allow proper migration of the particles to the preferred chemical environment. After the clear separation of the two phases, the upper one was carefully collected with help of a Pasteur pipette to avoid loss of the phase. Both, collected and remaining material were filtered, dried in an oven at 100°C, and weighed to obtain the floated mass and the sunk mass. This test was conducted in quadruplicate.

2.2.4. Sphericity test—permeametry

For permeametry experiments, three size fractions (+105 μm, −105 + 44 μm, −44 μm) were magnetically separated to render two samples: magnetic and nonmagnetic. After that, each sample (magnetic and nonmagnetic from final tailings) was packed in a small Büchner funnel, measuring 48.5mm in diameter and 23.3 mm in height. The packed funnel bed was inserted in a Kitassato glass, which had two lateral connections: (i) one was linked to a flowmeter coupled to a vacuum pump (200 mmHg); (ii) another went to a manometer for pressure loss measurements.

The permeametry tests were conducted by varying the suction flow from 0 to 5 $L.min^{-1}$. The relationship between pressure drop and flow allows the calculation of the permeametry constant (K), which is the parameter for calculating the sphericity (Ψ).

3. Results and discussion

Figures 2a and 2b shows the Fe and SiO_2 distributions in feed, concentrate, and tailing, respectively, of Conceição Itabiritos II plant, as a function of particle size. The higher percentage of iron contained in the flotation feed (57%) is concentrated in the particles < 30 μm. The iron particles higher than 150 μm represent only 3.9% of flotation feed and 1.1% of these particles were reported to the froth (tailings). On the other hand, the percentage of SiO_2 (55%) particles more expressive was found in the coarse size fractions (+150 μm) (Figure 2b). It was also observed that the SiO_2 particles recovery having −150 + 75 μm and −75 + 30 μm were very high (~96% and 99%, respectively).

Figures 3a and 3b shows the Fe and SiO2 distributions in feed, concentrate, and tailing, respectively, for Pico plant, as a function of particle size. It was observed that 12% of iron particles smaller than 30 μm floated. Pure hematite fine particles are mostly unfloatable (25%), as expected, and this significant percentage of particles (12%) that float is probably there due to hydrodynamic drag and entrainment processes and/or lack of depressant. It can be seen from Figure 3b that SiO_2 recovery in the concentrate was very low and the tailing contains mainly coarse SiO_2 particles.

Although we have conducted studies for samples acquired from feed, concentrate, and tailings, our major interest was in regard to the contents of iron-bearing minerals in the tailings, besides the size and shape of those minerals particles. Here, the iron minerals dealt with are basically hematite (Fe_2O_3) and magnetite (Fe_3O_4), and less importantly, the hydrated iron oxide goethite (FeO)OH. From now, to facilitate the reading, we shall assign the results as FTC (flotation tailings from Conceição Itabiritos II) and FTP (flotation tailing from Pico).

Silica, mostly present as quartz mineral is typically the most abundant contaminant for the iron ores, despite other minerals, which are present in much lower concentration. Figures 4a and 4b brings the iron and silica contents in the particle size fractions analyzed for both FTC and FTP. Not surprisingly, an inspection of the graphs reveals that the largest loss of iron, in terms of iron contents for both cases, was found in the finest fractions. The particles smaller than 44 μm comprise about 71% of all the iron lost in the flotation process of Conceição Itabiritos II plant and 85% for the Pico plant.

Considering all particle sizes, i.e. all the particles larger than 20 μm, it was found that FTP was composed basically of hematite (16%), quartz (80%), and goethite (3.7%). FTC was composed of hematite (14%), quartz (85%) and, in this case, the goethite represented only 0.7% of the minerals present in the tailings (Table 1). The larger amount of goethite in FTP shows the mineralogical difference between the iron ores extracted from these distinct mines.

Goethite is a very common mineral, and it can present several shapes and sizes, occurring mostly as a needle-like crystal. The presence of goethite makes the ore more friable increasing the amount of fines after grinding. Among the types of goethite, the earthy-like one is characterized by higher amounts of Al_2O_3 and SiO_2, together with other impurities (Santos and Brandão 2003). Differently, FTC was poorer than FTP in goethite contents rendering larger particles after the process as will be shown later in this work.

3.1. Liberation studies

Based on the already presented results, we concentrated our studies on the finest fractions, from where most of the iron

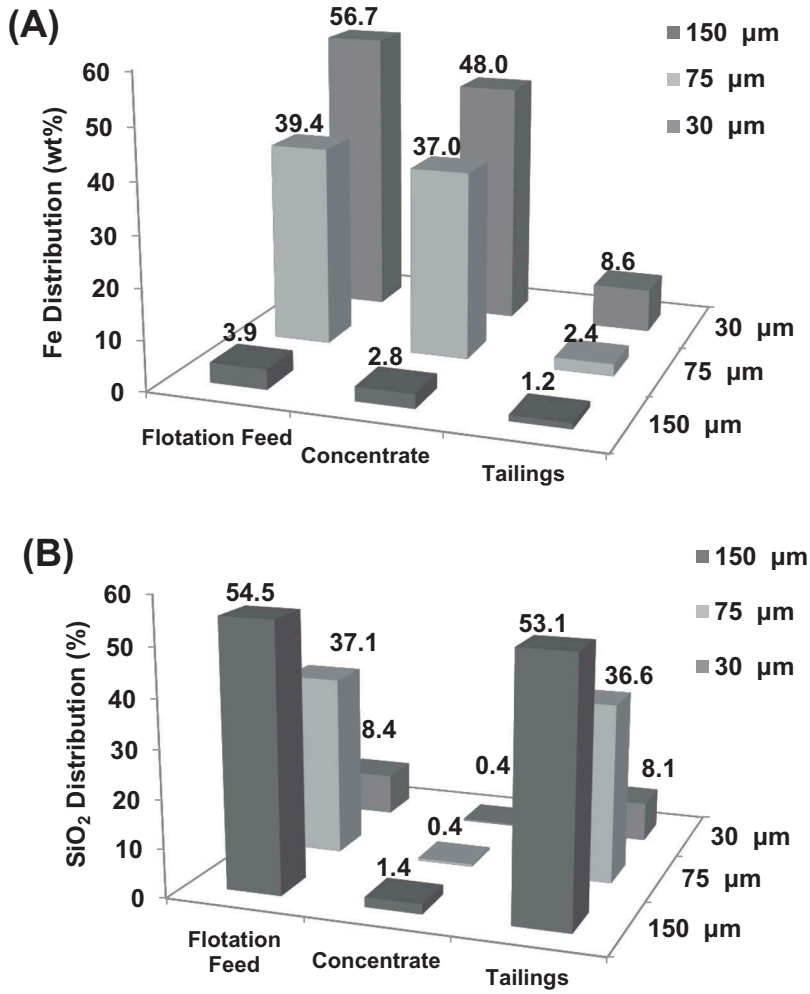

Figure 2. Metallurgical data as a function of particle size of Conceição Itabirito II plant. (a) Fe recovery (wt%) and (b) SiO_2 recovery (wt%).

minerals had been lost to the froth. There are some hypotheses, which should be contemplated in order to attribute the right source of loss, so the process can be accordingly tuned to minimize those losses.

The first possibility for the iron loss that must be taken into account is its association to other minerals forming composites that could have two or more mineral phases. If the mineral associated to the iron ore is susceptible to the action of the collector, there will be losses due to true flotation, according to the size of the phase containing the contaminant mineral. In the case of iron ore, the composite particles are mainly composed of quartz, besides hematite of course. Other minerals are always present, but in negligible quantities to interfere in the flotation process.

SEM micrographs associated with the MLA software data were used to evaluate the degree of liberation of the iron carrier particles. Figure 5 shows representative features of the images acquired from samples of FTC and FTP. Figure 5a (FTC) shows the image of a quartz particle having hematite associated as an inlaid particle. At Figure 5b (FTP), the typical features of goethite can be noticed, being more fibrous and porous than hematite or quartz particles. Tables 2 and 3 present the chemical composition, revealed by EDS, of the spots assigned with numbers in Figures 5a and 5b.

Table 4 presents the liberation class of hematite, and its associations, with respect to the particle size fraction for FTC. In this case, the particles having −44 + 20 µm presented complete liberation (96 wt%), since particles having 95 wt% liberation are considered liberated. The class of liberation decreases with the increase in the size of the particles, as expected. For the complete range of particle sizes, +20 µm, the liberation was 83 wt%.

The two-phase composites represented 17 wt% of the hematite with the second phase composed basically of quartz (13 wt%) or goethite (3.0 wt%). The three-phase composite was composed most often of hematite, quartz, and goethite. This last one representing only 0.4 wt%. These results raise the hypothesis of a depressant failure instead of collector's action over the quartz present on the composites.

Table 5 brings the results of the liberation studies for hematite, and its associations, with respect to the particle size fraction for FTP. According to these results, the finest size range particles were not liberated as observed for FTC. However, for the complete range of particles, the liberation was basically the same as found for FTC, 82 wt%. The binary composites represented 17 wt% of the hematite, being the second phase composed of goethite (13 wt%) and quartz (3.4%).

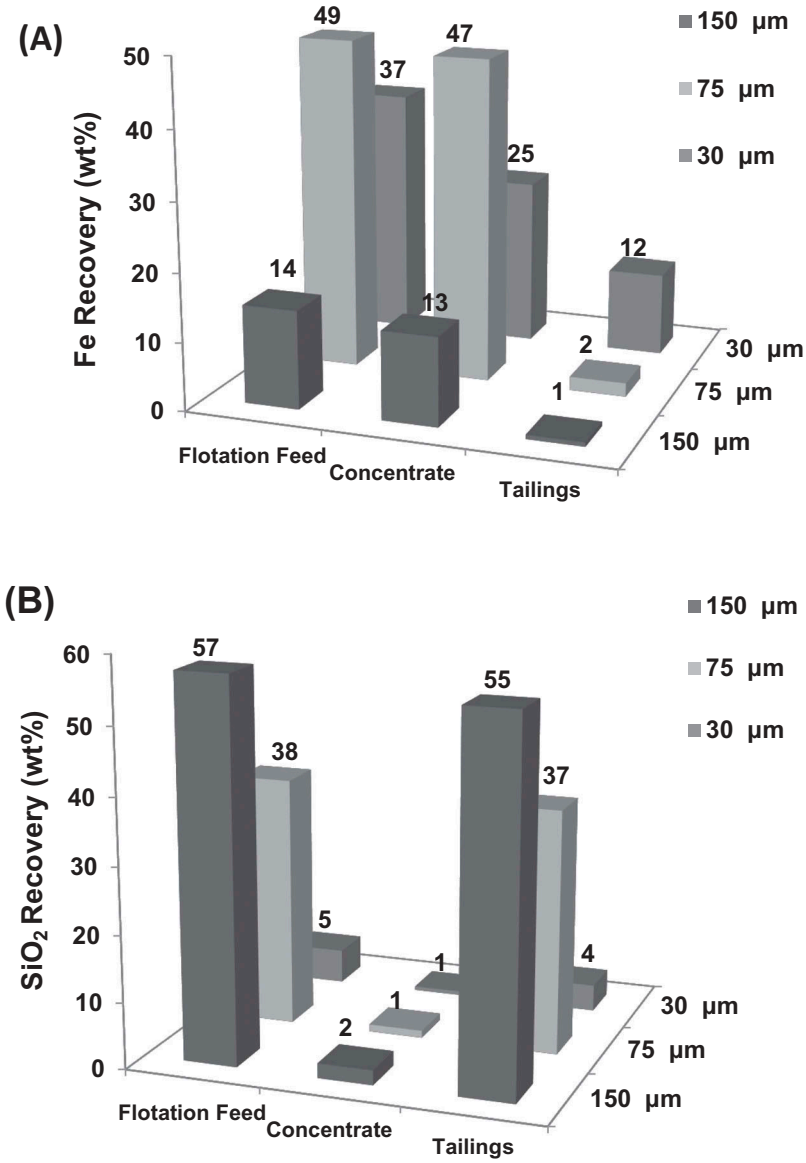

Figure 3. Metallurgical data as a function of particle size of Pico plant. (a) Fe recovery (wt%) and (b) SiO_2 recovery (wt%).

The finest FTP particles did not present the same liberation as FTC particles, being considered not liberated. Despite this, important information must be taken into account before assuming that true flotation has taken place due to lack of liberation. FTP binary composites were composed mainly of associations between hematite and goethite, which is also an iron-bearing mineral. Therefore, the goethite phase very likely did not interfere in the depression of the iron minerals because, at least in theory, the collector should exhibit basically the same behavior toward hematite and goethite. Moreover, possible effects arising from interactions between collector and such composites would be diminished for the amount of quartz is much lower than goethite.

For the finest particles, the results of the liberation studies for both, FTC and FTP, indicate a depressant failure in addition to hydrodynamic dragging for the loss of iron to the froth, instead of an interference of a silica collector provoking true flotation. On the contrary, for the coarser class size, which presented a degree of liberation around 10 wt%, the iron-bearing minerals losses could be attributed to the true flotation by means of the composite particles, where hematite is associated to quartz. Besides, larger particles are less affected by hydrodynamic dragging.

3.2. Permeametry—size and shape of particles

Beyond the size of the particles present in a flotation tank cell, their shape is also a crucial factor. Depending on its shape, a particle can markedly experience the entrainment mechanism due to the ascendant flux in the system, and to the energy released by the impeller within the flotation cell (Smith and Warren 1989). Thus, besides the size, it is essential to introduce the shape factor, given by the sphericity function of the particles, in the investigations about the loss of iron bearing minerals to the flotation froth. The sphericity can assume values between zero and one ($0 < \Psi \leq 1$), and as it gets closer to unity it gets more similar to a perfect sphere (Wadell 1935). A sphere is easier

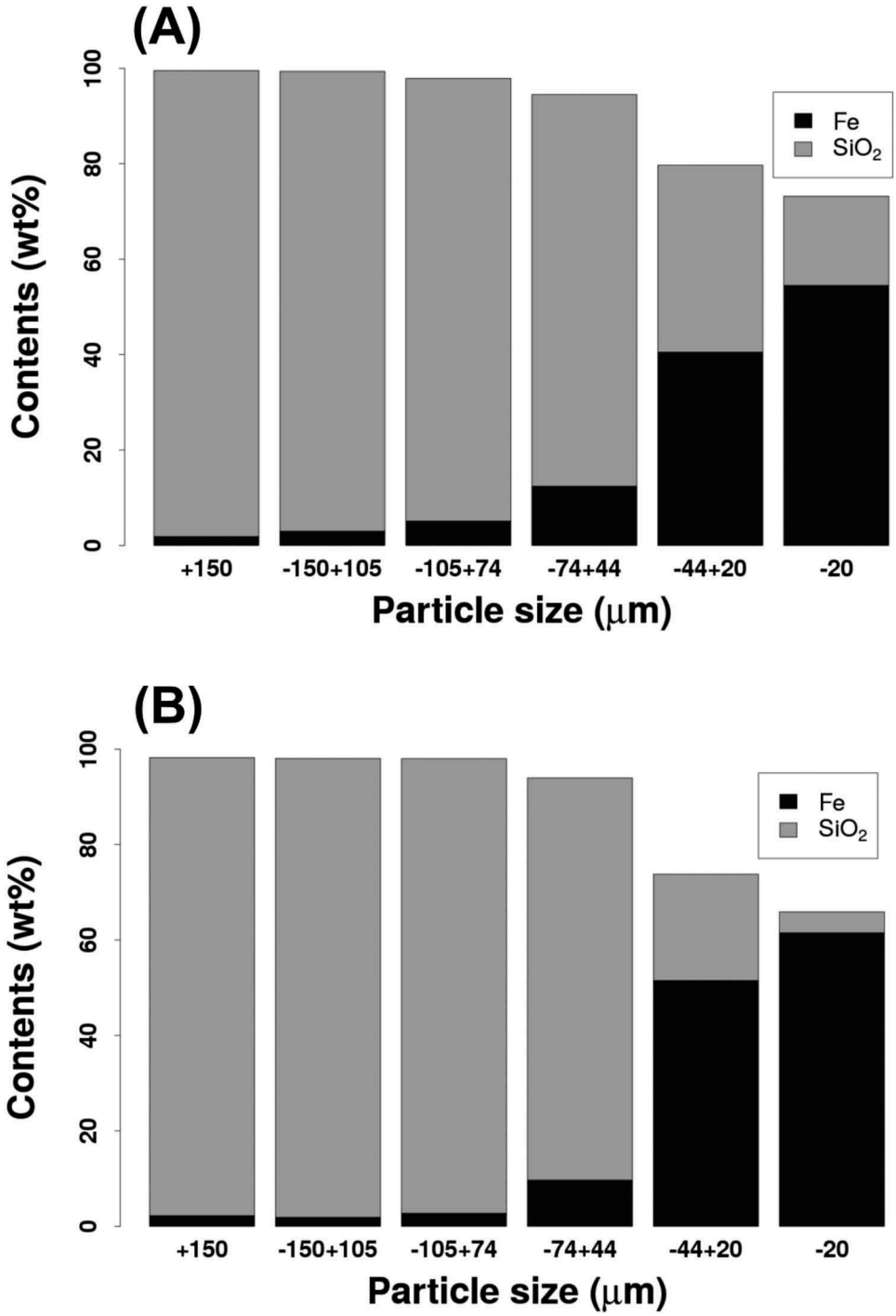

Figure 4. Contents of Fe and SiO_2 in the particles analyzed from (a) FTC and (b) FTP, according to their size distribution.

Table 1. Mineral composition of the tailings from the flotation process of Conceição Itabiritos II (FTC) and Pico (FTP) plants.

	FTC	FTP
Minerals	Total (+20 μm) (%)	Total (+20 μm) (%)
Hematite	14	16
Quartz	85	80
Goethite	0.7	3.7
Clay minerals	0.2	0.2
Others	0.1	0.1

to drag than a tetrahedron, for instance. Figure 6 illustrates some common shapes and the sphericity associated to them.

Considering very low Reynolds numbers, the pressure drop for the laminar air flow can be calculated by using the Kozeny-Carman relation (Equation 1) (McCabe et al. 2004):

$$\frac{\Delta P}{L} = \frac{72\lambda_1 \dot{V}_o \mu (1-\varepsilon)^2}{\Psi^2 D_{3,2}^2 \varepsilon^3} \quad (1)$$

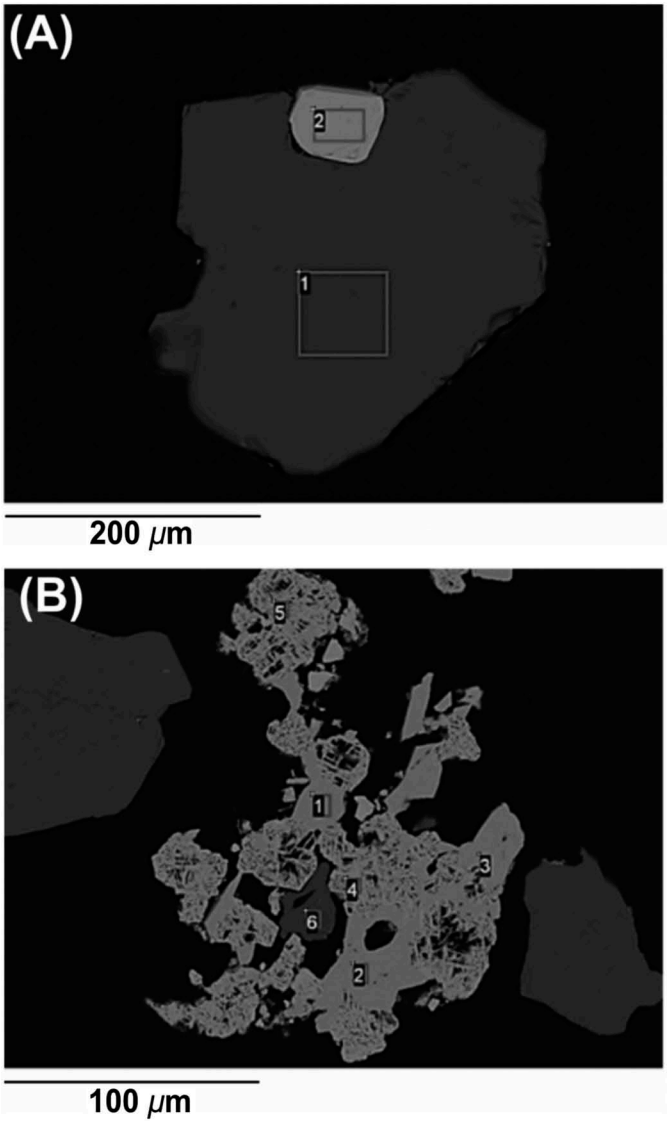

Figure 5. SEM micrographs acquired from representative samples of (a) FTC and (b) FTP. The regions assigned with numbers were chemically analyzed by EDS and their composition in terms of Fe, SiO_2, Al_2O_3, and P is shown in Tables 2 and 3.

Table 2. Chemical composition of the regions assigned in the SEM image acquired from FTC sample, shown at Figure 3a.

	Element/mineral grade (wt%)	
EDS region	Fe	SiO_2
1	–	100
2	68.7	–

Table 3. Chemical composition of the regions assigned in the SEM image acquired from FTP sample, shown at Figure 3b.

	Element/mineral grade (wt%)			
EDS region	Fe	SiO_2	Al_2O_3	P
1	57.7	1.45	1.97	–
2	57.3	1.44	2.34	0.11
3	57.8	1.54	2.00	–
4	63.4	0.52	–	–
5	63.0	0.71	0.44	–
6	–	100	–	–

Where, $\Delta P/L$ = press ure drop through a packed bed of length L; λ_1 = correction factor equal to 2.5, or 72 λ_1 = 180 (Mauri 2015); v_0' =average fluid velocity; μ = dynamic air viscosity; ε = porosity; Ψ = sphericity of particles; and $D_{3,2}$ = Sauter mean diameter of particles.

For a size distribution of particles, the permeability of a medium (K) can be determined by Equation 2, which is a rearrangement of Darcy's law (McCabe et al. 2004):

$$K = \frac{-\mu Q}{A\Delta P/L} \tag{2}$$

Where, K = permeametry constant; μ = dynamic air viscosity; Q = airflow rate; A = cross-sectional area of packed bed; $\Delta P/L$ = pressure drop through a packed bed of length L.

Using Equations 1 and 2, it is possible to calculate the sphericity (Ψ) according to Equation 3 (McCabe et al. 2004; Mauri 2015):

$$\Psi = \sqrt{\frac{180K(1-\varepsilon)^2}{D_{3,2}^2\varepsilon^3}} \tag{3}$$

Where, K = permeability of porous media, $D_{3,2}$ = Sauter mean diameter of particles, and ε = porosity of the column of particles. Tables 7 and 8 show the $D_{3,2}$ and sphericity results of hematite and quartz particles for FTC and FTP, respectively. *Note that Sauter's diameter was determined by laser diffraction in another experiment.*

In Tables 6 and 7, it is possible to notice that the sphericity increases more sharply for the finest particles (−44 μm), and it keeps almost constant for the two other size fractions, not showing a direct relation between $D_{3,2}$ and Ψ for these range of sizes. Unfortunately, it was impossible to determine the sphericity of the quartz particles for −44 μm of FTP samples because the pressure drop through a packed bed was too high for the experimental apparatus used.

The terminal velocity (TV) of the hematite particles was calculated following the method proposed by Concha and Barrientos (Concha and Barrientos, 1986) for nonspherical particles, and it takes into account the shape factor (sphericity) of the particles. Nonspherical particles have different behavior from spherical particles during sedimentation. Whereas spherical particles follow basically a vertical trajectory, the nonspherical ones rotate, vibrate, and describe a spiral path during their fall. Still according to Concha and Barrientos, the sphericity by itself is not enough to determine the shape of particles because there can be particles with same sphericity, but different shapes. However, they have proved that for isometric particles the sphericity can definitely discriminate their shapes.

For particles which have the same density and diameter, it is not a surprise that the terminal velocity is larger for particles that are more spherical. For Pico Mine, TV of tailings particles is higher than those from concentrate because particles of quartz (the main component in these tailings) have an intermediate shapes, i.e. neither needle nor spherical and it seems that floated much better.

The particle shape has a significant effect on the floatability of mineral and hence the detachment force of shaped particle is higher than that spherical particle (Xia 2017).

Table 4. Class of liberation and association forms of hematite, according to the particle size distribution, for FTC.

Hematite associations (wt%)	Particle size distribution (μm)						
	Total (+20)	+210	−210 + 150	−150 + 105	−105 + 74	−74 + 44	−44 + 20
Liberated	83	11	18	33	54	80	96
Composite (2 phases)	17	88	81	65	44	19	4.0
Composite (3 phases)	0.4	0.7	1.4	1.3	1.2	0.8	0.1

Table 5. Class of liberation and association forms of hematite, according to the particle size distribution, for FTP.

Hematite associations (wt%)	Particle size distribution (μm)					
	Total (+20)	+150	−150 + 105	−105 + 74	−74 + 44	−44 + 20
Liberated	82	8.3	19	53	76	87
Composite (2 phases)	17	67	67	40	21	13
Composite (3 phases)	1.2	25	14	6.9	2.5	0.1

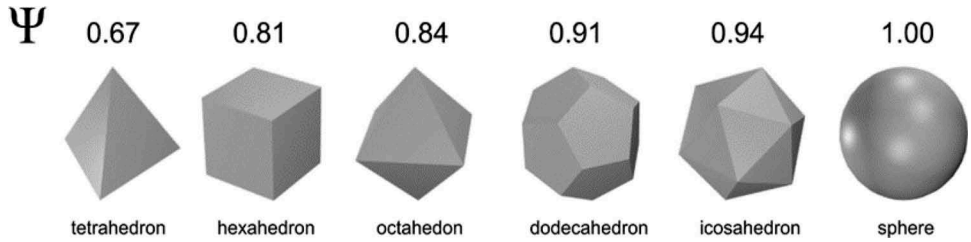

Figure 6. Relation between particle shapes and sphericity (ψ) values.

Table 6. Measured Sauter diameter ($D_{3,2}$) and calculated sphericity (ψ) of hematite particles, according to the size distribution for the tailings and concentrate from Conceição Itabiritos II plant.

Flotation product	Sample source	+105 μm		−105 + 44 μm		−44 μm	
		$D_{3,2}$	ψ	$D_{3,2}$	ψ	$D_{3,2}$	ψ
Tailings	Pico (FTP)	120.1	0.50	73.4	0.47	12.2	0.77
	Conceição (FTC)	55.8	0.56	53.4	0.52	16.2	0.72
Concentrate	Pico	103.4	0.37	59.6	0.48	36.1	0.50
	Conceição	157.3	0.32	65.8	0.51	29.8	0.57

Figure 7 compares the terminal velocities found for the hematite particles reporting to the tailings compared to the particles present in the concentrate, for three size fractions.

For both FTC and FTP we observed a reduction in TV with the decrease in the size of the particles, which was expected. The results obtained for the same size range of particles collected in different points of the flotation circuit, showed markedly different values for TV, which

Table 7. Measured Sauter diameter ($D_{3,2}$) and calculated sphericity (ψ) of quartz particles, according to the size distribution for the tailings and concentrate from Pico flotation plant.

Flotation product	Sample source	+105 μm		−105 + 44 μm		−44 μm	
		$D_{3,2}$	ψ	$D_{3,2}$	ψ	$D_{3,2}$	ψ
Tailings	Pico (FTP)	146.7	0.52	88.2	0.52	7.3	ND(*)
	Conceição (FTC)	166.8	0.58	76.5	0.57	13.3	0.95
Concentrate	Pico	276.2	0.31	ND(**)	ND(**)	ND(**)	ND(**)
	Conceição	309.0	0.53	91.1	0.46	20.8	ND(**)

(*) Not determined: with pecked bed highly compact, the apparatus was not able to measure the pressure drop.
(**) Not determined: the magnetic separation was not efficient.

Table 8. Fe and SiO_2 contents and distribution obtained from the finest particles (−44 μm) at the hydrophobic and hydrophilic phase in the two-liquid flotation experiments conducted for FTP.

Analyte	Final tail (−44 μm)		Hydrophilic phase		Hydrophobic phase	
	Contents (wt%)	Dist. (%)	Contents (wt%)	Dist. (%)	Contents (wt%)	Dist. (%)
Fe	57.6 ± 0.3	100.0	57.6 ± 0.3	97.7 ± 1.2	56.3 ± 1.0	2.3 ± 1.5
SiO_2	12.6 ± 0.2	100.0	12.7 ± 1.2	98.7 ± 1.0	6.5 ± 2.1	1.3 ± 1.0

strongly support that the particles reporting to the tailings present different behavior than the particles in the concentrate. This is especially true for FTC and corroborates for the validation of the hypothesis that the loss of hematite particles happens through hydrodynamic dragging. In FTC, we noticed that the difference between TV calculated for tailings and concentrate particles, for the fraction +105 μm, was very pronounced because of the difference in

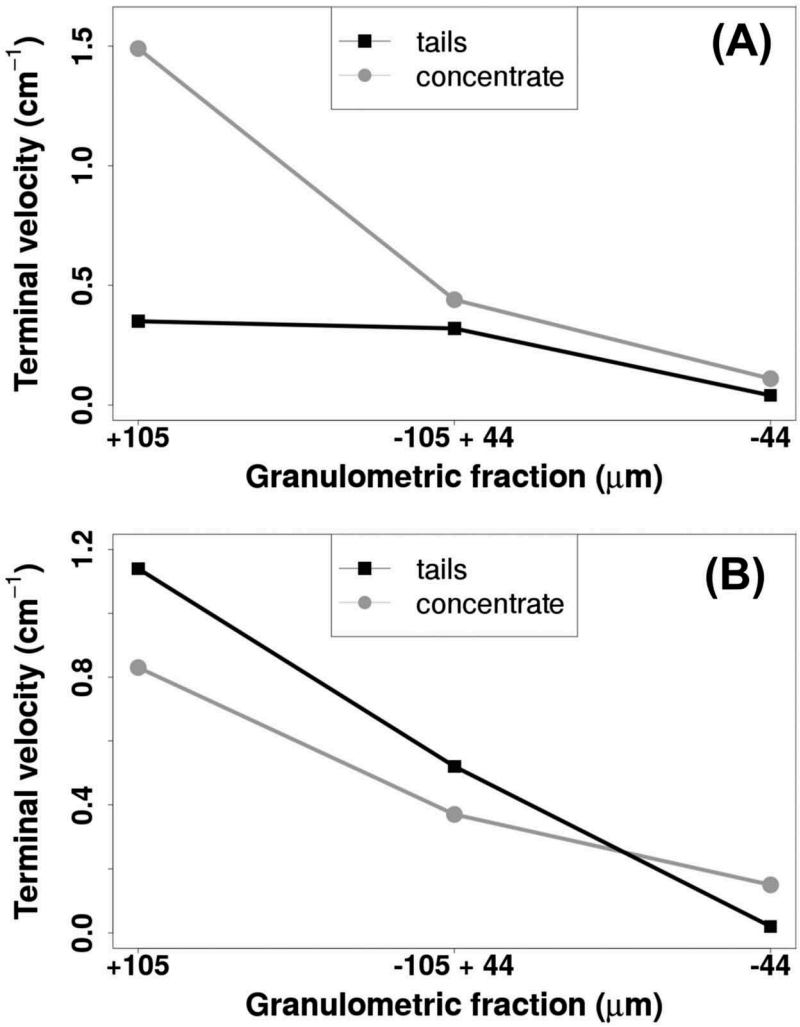

Figure 7. Terminal velocity (TV) calculated for the particles of hematite in the concentrate and final tailings of (a) Conceição Itabiritos II flotation plant and (b) Pico flotation plant, according to the size distribution.

particle size (concentrate = 55.8 μm; tailings = 157.3 μm, see Table 6), which decreases in finest (−105 μm) fractions. The same was not true for FTP where the hematite particles found in the tailings presented higher TV values for the two larger size fractions, becoming lower than the concentrate particles only for the finest particles. Those results are associated with the type of mineral and its associations, showing an intimate relation between terminal velocity and the mineralogical nature of the ore. Although the particles were the same size, they could contain more than one mineral phase (goethite) resulting in different density and TV values and to pertain for a same evaluated specific distribution of size.

3.3. Hydrophobicity of the particles

According to the results acquired in the permeametry experiments, the fine particles could have reached the froth via hydrodynamic dragging, becoming entrapped in the lamellae, as explained for the entrainment phenomenon. However, it is necessary to evaluate the chemical nature of the particles' surface to ensure if some failure during the chemical processes within the froth flotation were effective or not. By chemical processes we mean, for instance, the depression of iron-bearing particles by starch, or even the collection of quartz particles.

Two-liquid flotation, as already explained in the introduction of this work, is a separation method that gives quick answers about the hydrophobicity/hydrophilicity of small particles. By weighing the contents of the two phases resulting from the experiment, one can make qualitative conclusions about the surface properties of the minerals. The chemical analysis of each phase enhances the quality of the results from qualitative to semiquantitative. Thus, improving the reliability of the results.

Tables 8 and 9 present the results acquired from the two-liquid flotation experiments conducted for the particles of the size range

Table 9. Fe and SiO_2 contents and distribution obtained from the finest particles (−44 μm) at the hydrophobic and hydrophilic phase in the two-liquid flotation experiments conducted for FTC.

	Final tail (−44 μm)		Hydrophilic phase		Hydrophobic phase	
Analyte	Contents (wt%)	Dist. (%)	Contents (wt%)	Dist. (%)	Contents (wt%)	Dist. (%)
Fe	47.9 ± 0.9	100.0	43.0 ± 1.4	34.6 ± 2.4	51.0 ± 0.8	65.4 ± 2.4
SiO_2	28.2 ± 1.0	100.0	34.9 + 1.6	47.6 ± 2.2	24.1 ± 0.8	52.1 ± 2.2

−44 μm from FTC and FTP, respectively. As the experiment is completed, the upper phase is composed of the isooctane and the hydrophobized particles, and the lower phase, together with the damped material corresponds to the hydrophilic particles (Figure 8).

In principle, the iron present in the tailings should be hydrophilic thus it should be collected from the lower phase. The hydrophilicity of iron-bearing particles confirms the effectiveness of the depression process by starch. The iron-containing particles reporting to the upper layer reached the tailings (froth phase) either by hydrodynamic dragging or depressant failure. In this last case, the cause was an insufficient addition or inefficiency of the depression agent.

Beginning with FTP, according to Table 8, the recovery of iron from the upper hydrophobized phase was 2.30% whereas 97.7% of the Fe remained in the hydrophilic phase. Regarding quartz, 1.30% was recovered from the hydrophobic upper phase, and 98.7% of this mineral remained in the lower phase being considered hydrophilic. Combining these results with the permeametry results, it can be suggested that, the finest particles of hematite reached the froth phase by hydrodynamic dragging. Fine particles of quartz, in the same way, reported to the tailings also via hydrodynamic dragging, once they were not hydrophobic, as proven by their scarce presence in the hydrophobic phase.

The analysis of the data collected from FTC samples showed a different behavior. As shown in Table 9, the hydrophobic upper phase presented an iron recovery of 65.4%, whereas hydrophilic lower phase presented Fe recovery of 34.6%. This means that there were hydrophobic hematite particles, thus they were not successfully depressed. For quartz, the hydrophobic particles corresponded to 52.1% and hydrophilic particles to 47.6%. Those results show that, for FTC, fine particles of hematite could have reached the froth not only by hydrophobic dragging but also by true flotation. Moreover, a larger amount of hematite particles underwent true flotation than quartz particles. Differently from FTP, where the principal way of losing iron-bearing minerals to the froth was found to be the hydrodynamic dragging, the hematite present in FTC reached the froth by true flotation means, probably due to inefficiency in the depression process, besides the hydrodynamic dragging that seems to take place in both cases.

4. Conclusion

In this work, iron ores coming from two different mines and their flotation plants were the subject of study in order to evaluate if the loss of iron-bearing minerals to the tailings happened predominantly due to hydrodynamic dragging or true flotation, in the reverse cationic flotation process. The results obtained from the separation method called two-liquid flotation together with permeametry and liberation studies, for the finest particles (−44 μm), allowed us to conclude that the loss of iron-bearing minerals occurred by different means for the two flotation circuits analyzed. For the FTC, flotation tailings from Conceição Itabiritos II, the finest particles were considered liberated; therefore, the loss did not occur due to the presence of composite particles. In this case, the loss happened through true flotation in addition to hydrodynamic dragging. True flotation probably occurred due to a failure in the depression process of hematite with starch. For FTP, flotation tailings from Pico, the finest particles did not present the same degree of liberation shown by FTC, being considered not liberated. The binary composite particles, in this case, were mainly composed of hematite and goethite. As goethite should display the same behavior of hematite toward the depressant (starch) and the quartz collector, the loss of iron-bearing minerals to the tailings probably did not occur due the presence of such composites. For the FTP, two-liquid flotation showed that the majority of iron-bearing particles lost to the froth phase got there via hydrodynamic dragging, once nearly all the iron-bearing particles remained in the hydrophilic phase. For the FTC, 65.4% of hematite is recovered in the hydrophobic phase demonstrating that the loss of iron minerals was predominantly due to a true flotation. True flotation probably took place because of depression failure.

In both cases, two-liquid flotation was crucial to assess the results, providing fast and reproducible results and operating with simple glassware and equipment. This method could be easily applied in concentrator premises to provide quick evaluations for the iron ore depression efficiency.

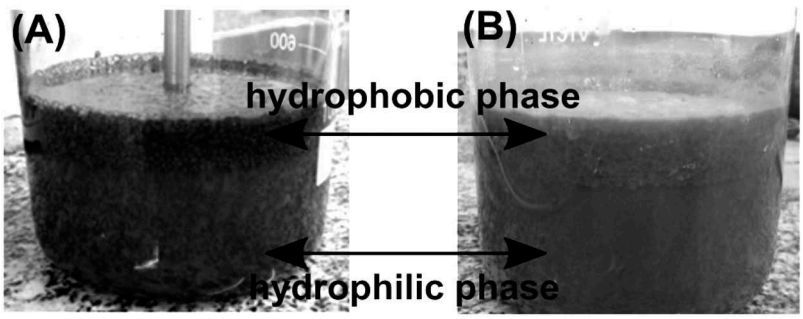

Figure 8. Typical appearance of the two phases during the resting time before the collection of the phases' contents of (a) FTC and (b) FTP. Note the difference in the color of the ores, especially in the upper phase, where FTP presents the typical color for goethitic minerals.

Acknowledgment

The authors acknowledge Vale S/A for the samples and technical support.

Disclosure statement

The authors report no conflicts of interest. The authors alone are responsible for the content and writing of the article.

ORCID

André S. Braga http://orcid.org/0000-0002-2558-276X

References

Arbiter, N., Harris, C. C., and Yap., R. F., 1976, "The air flow number in flotation machine scale-up." *International Journal of Mineral Processing*, 3. pp. 257–280.

Chau, T. T., 2009, "A review of techniques for measurement of contact angles and their applicability on mineral surfaces." *Minerals Engineering*, 22(3). pp. 213–219.

Concha, F., and Barrientos, A., 1986, "Settling velocities of particulate systems 4. Settling of nonspherical isometric particles." *International Journal of Mineral Processing*, 18(3). pp. 297–308.

Dowling, E. C., Hebbard, J., Eisele, T. C., and Kawatra, S. K., 2000, Processing of Iron Ore by Reverse Column Flotation, In *Proceedings of the XXI International Mineral Processing Congress*, (P. Massaci, Ed.), Amsterdam: Elsevier Ed., pp. 163–170.

Eisele, T. C., and Kawatra, S. K., 2007, "Reverse Column Flotation of Iron Ore." *Minerals and Metallurgical Processing*, 24(2). pp. 61–66.

Eriksson, M., Nyström, C., and Alderborn, G., 1990, "Evaluation of a permeametry technique for surface area measurements of coarse particulate materials." *International Journal of Pharmaceutics*, 63(3). pp. 189–199.

Gomes, M. A., Pereira, C. A., and Peres, A. E. C., 2011, "Caracterização tecnológica de rejeito de minério de ferro." *Rem: Revista Escola de Minas*, 64(2). pp. 233–236.

Gomes, R. B., Tomi, G. D., and Assis, P. S., 2015, "Impact of quality of iron ore lumps on sustainability of mining operations in the Quadrilatero Ferrifero Area." *Minerals Engineering*, 70. pp. 201–206.

Kawatra, S. K., and Eisele, T. C., 1987, Column Flotation of Coal, In *Fine Coal Processing*, (S. K. Mishra and R. R. Klimpel, Eds.), Park Ridge: Noyes Publications, pp. 414–429.

Kocabağ, D., and Güler, T., 2007, "Two-liquid flotation of sulphides: an electrochemical approach." *Minerals Engineering*, 20. pp. 1246–1254.

Lima, N. P., Souza Pinto, T. C., Tavares, A. C., and Sweet, J., 2016, "The entrainment effect on the performance of iron ore reverse flotation." *Minerals Engineering*, 96–97. pp. 53–58.

Lima, N. P., Valadão, G. E. S., and Peres, A. E. C., 2013, "Effect of amine and starch dosages on the reverse cationic flotation of an iron ore." *Minerals Engineering*, 45. pp. 180–184.

Mauri, R., 2015, *Transport Phenomena in Multiphase Flows in Fluid Mechanics and Its Applications*, Vol. 112 vol., Switzerland: Springer Ed., pp. 459.

McCabe, W. L., Smith, J. C., and Harriott, P., 2004, *Units Operation of Chemical Engineering*, 7th edition, New York: McGraw-Hill Ed., pp. 1140.

Neethling, S. J., and Cilliers, J. J., 2009, "The entrainment factor in froth flotation: model for particle size and other operating parameter effects." *International Journal of Mineral Processing*, 93. pp. 141–148.

Otsuki, A., and Dodbiba, G., 2007, "Heterocoagulation of fine particles in polar organic solvent." *Materials Transactions*, 48(5). pp. 1095–1104.

Pavlovic, S., and Brandão, P. R. G., 2003, "Adsorption of starch, amylose, amylopectin and glucose monomer and their effect on the flotation of hematite and quartz." *Minerals Engineering*, 16(11). pp. 1117–1122.

Peres, A. E. C., and Correa, M. I., 1996, "Depression of iron oxides with corn starches." *Minerals Engineering*, 9(12). pp. 1227–1234.

Ross, V. E., 1991, "The behaviour of particles in flotation froths." *Minerals Engineering*, 4(7). pp. 959–974.

Santos, L. D., and Brandão, P. R. G., 2003, "Morphological varieties of goethite in iron ores from Minas Gerais, Brazil." *Minerals Engineering*, 16(11). pp. 1285–1289.

Schubert, H., 2008, "On the optimization of hydrodynamics in fine particle flotation." .*Minerals Engineering*, 21(12–14). pp. 930–936.

Schulz, N. F., 1974, "Measurement of surface areas by permeametry." *International Journal of Mineral Processing*, 1(1). pp. 65–79.

Selmi, M., Lagoeiro, L. E., and Endo, I., 2009, "Geochemistry of hematitite and itabirite, Quadrilátero Ferrífero, Brazil." *Rem: Revista Escola de Minas*, 62(1). pp. 35–43.

Shean, B. J., and Cilliers, J. J., 2011, "A review of froth flotation control." *International Journal of Mineral Processing*, 100. pp. 57–71.

Smith, P. J., and Warren, L. J., 1989, Entrainment of particles into flotation froth, In *Frothing in Flotation*, (J. S. Laskowski, Ed.), New York: Gordon and Breach Science Publishers, pp. 123–144.

Souza Pinto, T. C., Lima, O. A., and Leal Filho, L. S., 2009, "Sphericity of apatite particles determined by gas permeability through packed beds." *Minerals & Metallurgical Processing*, 26. pp. 105–108.

Souza Pinto, T. C., Slatter, P. T., Matai, P. H., and Leal Filho, L. S., 2016, "The influence of hematite particle shape on stratification in pipe flow." *Powder Technology*, 302. pp. 75–80.

Wadell, H., 1935, "Volume, shape and roundness of quartz particles." *Journal of Geology*, 43(3). pp. 250–280.

Wang, L., Peng, Y., Runge, K., and Bradshaw, D., 2015, "A review of entrainment: mechanisms, contributing factors and modeling in flotation." *Minerals Engineering*, 70. pp. 77–91.

Wiese, J., Becker, M., Yorath, G., and O'Connor, C., 2015, "An investigation into the relationship between particle shape and entrainment." *Minerals Engineering*, 83. pp. 211–216.

Xia, W., 2017, "Role of particle shape in the floatability of mineral particle: an overview of recent advances." *Powder Technology*, 317. pp. 104–116.